Journal of
Applied Crystallography
ISSN 1600-5767

NXFit: a program for simultaneously fitting X-ray and neutron diffraction pair-distribution functions to provide optimized structural parameters

David Pickup, Robert Moss and Robert Newport

J. Appl. Cryst. (2014). **47**, 1790–1796

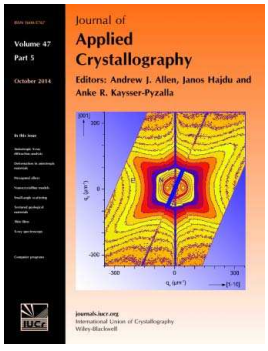

Journal of
Applied Crystallography
ISSN 1600-5767

Received 4 April 2014
Accepted 8 August 2014

NXFit: a program for simultaneously fitting X-ray and neutron diffraction pair-distribution functions to provide optimized structural parameters

David Pickup,* Robert Moss and Robert Newport

School of Physical Sciences, Ingram Building, University of Kent, Canterbury, Kent CT2 7NH, England. Correspondence e-mail: dmp@kent.ac.uk

NXFit is a program for obtaining optimized structural parameters from amorphous materials by simultaneously fitting X-ray and neutron pair-distribution functions. Partial correlation functions are generated in Q space, summed and Fourier transformed for comparison with the experimental data in r space. *NXFit* uses the Nelder–Mead method to vary a set of 'best guess' parameters to achieve a fit to experimentally derived data. The output parameters from *NXFit* are coordination number, atomic separation and disorder parameter for each atomic correlation used in the fitting process. The use of *NXFit* has been demonstrated by fitting both X-ray and neutron diffraction data from two quite different amorphous materials: a melt-quenched $(Na_2O)_{0.5}(P_2O_5)_{0.5}$ glass and a $(TiO_2)_{0.18}(SiO_2)_{0.82}$ sol–gel.

1. Introduction

Since the atomic structure of materials often plays a key role in determining their physical properties, knowledge of how the atoms are arranged is fundamental to materials science. Diffraction has become an important tool for determining the atomic scale structure of materials, and advanced instrumentation has made the collection of high-quality data possible. However, analysis and interpretation of that data can still be difficult, particularly where the material has a complicated structure and/or multiple components. There are various approaches to fitting data from crystalline materials, the most common of which is Rietveld (1969) refinement, which can be applied to both X-ray and neutron diffraction data. Fitting diffraction data from amorphous materials is more problematic, and different processes have been formulated. One method is to prepare atomistic models and to refine these against the experimentally obtained diffraction pattern. This is the approach adopted in reverse Monte Carlo (RMC) modelling (McGreevy & Pusztai, 1988; McGreevy, 2001) and, more recently, in empirical potential structure refinement (Soper, 2001, 2005). Another method is to calculate the model, for example using molecular dynamics simulations (Alder & Wainwright, 1959; Cormack & Cao, 1996), and then compare aspects of this model with those from the experimental data.

An alternative approach is to convert the diffraction data into a real-space pair-distribution function by Fourier transformation and fit this function with a series of peaks that simulate the correlations between pairs of atoms. This method has been applied successfully to both crystalline (Hannon *et al.*, 2008) and disordered materials (Hoppe *et al.*, 1995). An advantage of this method is that it is possible to simultaneously fit X-ray and neutron data from the same sample using a single set of structural parameters. This feature is particularly useful when fitting data where there are a large number of overlapping correlations (in a multicomponent glass for example), because the relative contribution of each atomic pair to the data is different for X-rays and neutrons. X-rays interact with the electrons in the atoms and preferentially pick out high-Z elements, whereas neutrons interact with the nuclei in the sample and the scattering strength does not exhibit a monotonic trend with atomic number.

Whilst programs such as *PDFfit2* and *PDFgui* (Farrow *et al.*, 2007) are available to fit theoretical three-dimensional structures to atomic pair-distribution functions from crystalline materials, the modelling of such data from amorphous materials is more difficult. The program presented here, *NXFit*, automates the fitting of pair-distribution functions from amorphous materials and is capable of fitting X-ray and neutron scattering data simultaneously. The user specifies a set of initial structural parameters, atom types and distances, coordination numbers, and disorder parameters to describe the correlations between the pairs of atoms present in the structure. These are used to generate partial correlation functions in Q space, which are summed before Fourier transformation for comparison with the experimental pair-distribution function. The parameters are then refined until a satisfactory fit to the experimental data is achieved. The advantage of generating the simulation in Q space is that, provided the same Fourier transform range is used for the data and the simulation, truncation effects due to the finite range of the data in Q space can be ignored.

The application of *NXFit* is demonstrated by fitting both X-ray and neutron diffraction data from two very different amorphous materials: a sodium metaphosphate glass prepared by melt quenching a molten mixture of oxides and a mixed TiO_2–SiO_2 glass prepared by a low-temperature sol–gel route.

2. Theory and data analysis

In order to obtain structural information from neutron diffraction data, it is first necessary to perform corrections for background scattering, absorption and multiple scattering to determine the differential cross section (Hannon *et al.*, 1990):

$$\frac{d\sigma}{d\Omega} = i(Q) + I_S(Q), \quad (1)$$

where $Q = 4\pi \sin\theta/\lambda$ (2θ is the scattering angle and λ is the neutron wavelength), $I_S(Q)$ is the self-scattering and $i(Q)$ is the structure-dependent part of the data. The self-scattering term can be calculated (Wright, 1985) and subtracted to yield the interference function $i(Q)$.

Similarly, with X-ray diffraction the measured scattering intensity is corrected for polarization and absorption effects, background scattering, and Compton scattering to yield $d\sigma/d\Omega$. The structure-dependent interference function $i(Q)$ can then be extracted from $d\sigma/d\Omega$ (Pings & Waser, 1968):

$$i(Q) = \frac{d\sigma}{d\Omega} - \sum_{i=1}^{n} c_i f_i(Q)^2, \tag{2}$$

where f_i are the Q-dependent atomic scattering factors, c_i are the atomic fractions of the components and n is the number of atom types.

When fitting neutron and X-ray data simultaneously, it is beneficial to normalize each $i(Q)$ to have the same units before transformation to the real-space pair-distribution function. This can help prevent scaling problems and is required when using *NXFit*. If $a(Q)$ is introduced to represent either the neutron scattering length b or the X-ray scattering factor $f(Q)$, the total scattering structure factor is defined as (Keen, 2001)

$$S(Q) - 1 = i(Q) \Big/ \left[\sum_{i=1}^{n} c_i a_i(Q)\right]^2. \tag{3}$$

When dealing with X-ray data, the denominator of equation (3) is sometimes referred to as the sharpening function. Some workers use $[\sum_{i=1}^{n} c_i f_i(Q)]^2$ as the sharpening function, and others use $\sum_{i=1}^{n} c_i f_i(Q)^2$. Care must be taken to use the former when preparing data to be used with *NXFit*.

Useful structural information can be extracted by Fourier transformation of the structure factor to the total correlation function $T(r)$:

$$T(r) = 4\pi\rho_0 r + (2/\pi) \int_0^\infty Q[S(Q) - 1]M(Q) \sin(rQ)\, dQ, \tag{4}$$

where ρ_0 is the macroscopic number density, r the scalar distance between pairs of atoms and $M(Q)$ a modification function that takes into account that data cannot be collected over an infinite Q range. The simplest modification function is a step function, which is unity for $Q \leq Q_{max}$ and zero for $Q > Q_{max}$. This is equivalent to using no modification function at all and results in termination ripples on either side of the peaks in $T(r)$. Such termination ripples can be suppressed by using a modification function that slopes more gently to zero. The two that can be used in conjunction with *NXFit* are the Lorch (1969) function,

$$M_{Lorch}(Q) = \begin{cases} \sin(\Delta r Q)/\Delta r Q, & Q \leq Q_{max}, \\ 0, & Q > Q_{max}, \end{cases} \tag{5}$$

and the Hanning window function (Yarker *et al.*, 1986),

$$M_{Hanning}(Q) = \begin{cases} [1 + \cos(\Delta r Q)]/2, & Q \leq Q_{max}, \\ 0, & Q > Q_{max}, \end{cases} \tag{6}$$

where $\Delta r = \pi/Q_{max}$. Both have the effect of reducing termination ripples but at the expense of real-space resolution.

$T(r)$ can be described as a weighted sum of the partial correlation functions $t_{ij}(r)$:

$$T(r) = \sum_{i,j}^{n} c_i a_i(Q) a_j(Q) t_{ij}(r), \tag{7}$$

where the i, j summations are each over the elements in the sample. The weighted partial correlation functions manifest themselves as peaks in $T(r)$, with positions corresponding to interatomic distances between pairs of atoms and areas that represent the coordination numbers of these atomic pairs. In disordered materials all but the peaks representing the nearest-neighbour distances overlap with other peaks, and it becomes necessary to deconvolve the contributions from each atomic pair to yield structural information. This can be achieved using an approach based on the Debye scattering equation, which gives the average scattering from an array of atoms that takes all orientations in space (Warren, 1990):

$$i(Q) = \sum_{m,n} a_m(Q) a_n(Q) \sin(Qr_{mn})/(Qr_{mn}), \tag{8}$$

where m and n are the atoms in the array and r_{nm} the distances of each atom from every other atom.

By ascribing a Gaussian-type distribution to the interatomic distances, we can derive the pair function $p_{ij}(Q)$, which can be used to model each $t_{ij}(r)$ in Q space:

$$p_{ij}(Q) = \frac{N_{ij} w_{ij}(Q)}{c_j} \frac{\sin(QR_{ij})}{QR_{ij}} \exp\left(\frac{-Q^2\sigma_{ij}^2}{2}\right), \tag{9}$$

where N_{ij}, R_{ij} and σ_{ij} are the coordination number, atomic separation and disorder parameter (*i.e.* a measure of the thermal and static disorder), respectively, of atom type i relative to atom type j. The weighting factors w_{ij} are the probe-dependent quantities given by

$$w_{ij} = \frac{(2 - \delta_{ij}) c_i c_j a_i(Q) a_j(Q)}{\left[\sum_{i=1}^{n} c_i a_i(Q)\right]^2}, \tag{10}$$

where δ_{ij} is the Kronecker delta function (*i.e.* $\delta_{ij} = 1$ for $i = j$ or $\delta_{ij} = 0$ for $i \neq j$) and a_i is the probe-dependent term: either the Q-independent neutron scattering length b or the Q-dependent X-ray scattering factor $f(Q)$.

Individual $p_{ij}(Q)$ functions can be calculated for each pair of atoms, summed and Fourier transformed for comparison with $T(r)$ (Bruni *et al.*, 1995). The advantage of simulating $T(r)$ in this way is that the Fourier transformation is the same for both the data and the fit, negating the effects of the finite upper limit of Q, providing the same Q range and modification function is used in each case. The values of N_{ij}, R_{ij} and σ_{ij} are varied to optimize the fit to the experimental data: the use of *NXFit* provides a convenient method to achieve this optimization.

3. Program details

NXFit was written in MATLAB (The MathWorks, Natick, MA, USA) but has been compiled to run alongside the MATLAB Compiler Runtime (MCR) on an end-user's machine. Both Linux and Windows versions are available free of charge to academic users at http://www.kent.ac.uk/physical-sciences/soft/nxfit/nxfit.html. *NXFit* uses the Nelder–Mead (also known as the 'downhill' or 'amoeba') method, which is a commonly used nonlinear optimization algorithm, to vary a set of 'best guess' parameters to achieve a fit to experimentally derived data. The scheme was developed by Nelder & Mead (1965) and is a numerical method for minimizing an objective function in an N-dimensional space. The method uses the concept of a simplex, which is a polytope with $N + 1$ vertices. For example, in one dimension the polytope is a line segment, in two dimensions it is a triangle and in three dimensions it is a tetrahedron. As the dimensionality of the problem increases, the polytope becomes more complex. The Nelder–Mead simplex method finds, approximately, the solution to a problem with N variables when the objective function

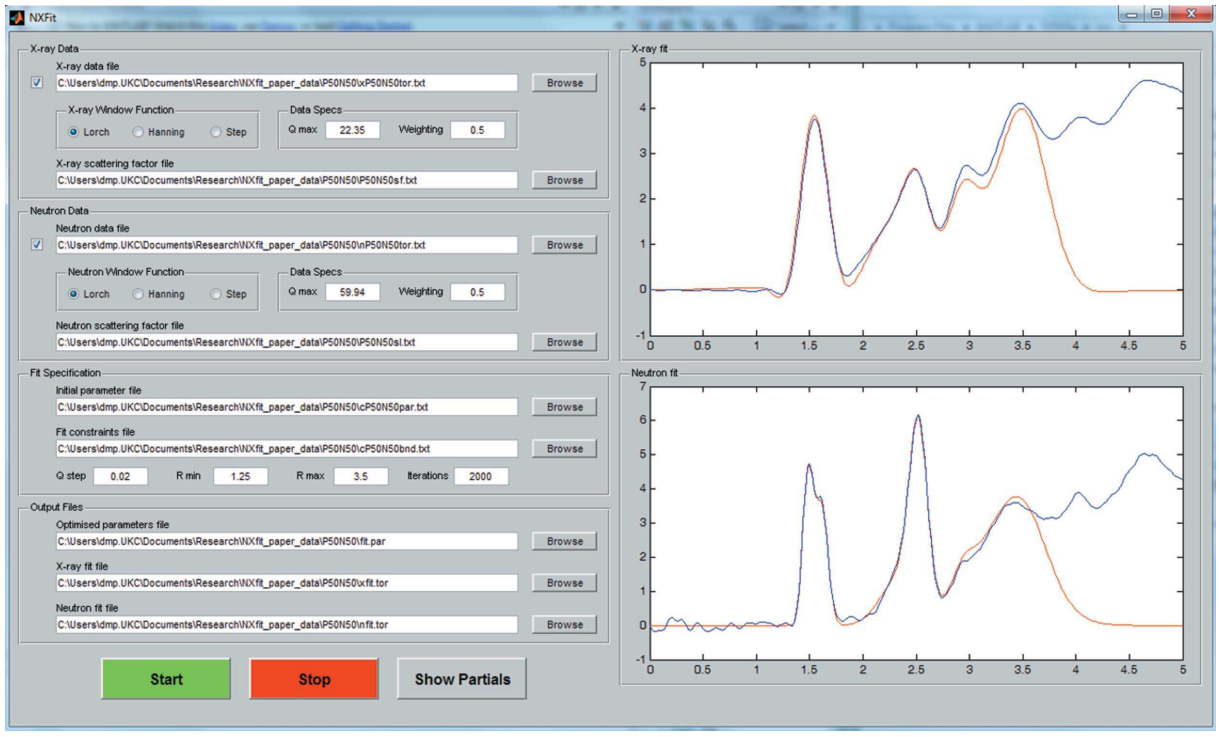

Figure 1
Initialized *NXFit* GUI with all fields completed and ready to start the simulation. Plots in the right-hand panels show the experimental data (blue lines) and simulated fits (red lines)

varies smoothly. In the case of *NXFit*, the objective function is the combination of peaks that are being used to simulate the experimental $T(r)$ and the value of interest to the optimization routine is the least-squares fit index, FI:

$$\mathrm{FI} = \sum_{r=R_{\min}}^{r=R_{\max}} \left\{ w^{\mathrm{X}} \left[T_{\mathrm{E}}^{\mathrm{X}}(r) - T_{\mathrm{S}}^{\mathrm{X}}(r) \right]^2 + w^{\mathrm{N}} \left[T_{\mathrm{E}}^{\mathrm{N}}(r) - T_{\mathrm{S}}^{\mathrm{N}}(r) \right]^2 \right\}, \qquad (11)$$

where the subscripts E and S denote, respectively, the experimental and simulated correlation functions, the superscripts X and N refer to the type of data (*i.e.* either X-ray or neutron), $R_{\min}$ and $R_{\max}$ define the range over which the data is simulated, and w^{X} and w^{N} are weighting factors that can be used to preferentially weight one data set over the other during the fitting process (see below). The value of FI is determined at each vertex of the polytope. In the simplest case, the point that yields the worst FI value is rejected and a new test point is developed by reflecting the simplex through the centroid of the remaining N points. If the new point is much better, then the simplex stretches out exponentially along this line. However, if the new point is not much better than the original test point, then the algorithm assumes that it is stepping across a valley and shrinks the simplex towards the best point. An occasional problem of multidimensional optimization algorithms is that they can become stuck in local minima because of the collapse of the simplex. The Nelder–Mead method is not immune in this regard (McKinnon, 1998). The standard approach to handling this is to arrange a new simplex starting from the current best parameter values. There are alternatives to Nelder–Mead, such as the flexible polyhedron method, but this tends to make a large number of unnecessary steps in regions of little interest and takes longer to converge on a solution.

In *NXFit* the Nelder–Mead method is implemented through the MATLAB function *fminsearch*, which uses the simplex algorithm as described by Lagarias *et al.* (1998). The behaviour of the simplex during the optimization is controlled by the parameters α, γ, ρ and σ, which are the reflection, expansion, contraction and shrink coefficients, respectively. The function *fminsearch* uses values of $\alpha = 1$, $\gamma = 2$, $\rho = 0.5$ and $\sigma = 0.5$.

The Nelder–Mead routine alone does not have any capacity to include constraints, but in order to fit experimental diffraction data it is necessary to constrain the fitting parameters to avoid nonphysical solutions. Upper and lower bounds are implemented with a wrapper function called *fminsearchcon*,[1] which sits on top of *fminsearch* and uses a sinusoidal transformation of the parameters:

$$y(i) = \mathrm{LB}(i) + \tfrac{1}{2}[\mathrm{UB}(i) - \mathrm{LB}(i)]\{\sin[z(i)] + 1\}, \qquad (12)$$

where $y(i)$ is the real parameter, $z(i)$ is the transformed parameter, and $\mathrm{UB}(i)$ and $\mathrm{LB}(i)$ are the upper and lower bounds of $y(i)$, respectively. It is clear from equation (12) that if $z(i)$ is unconstrained and can have any value $-\infty \leq z(i) \leq +\infty$, $y(i)$ is restricted to the range $\mathrm{LB}(i) \leq z(i) \leq \mathrm{UB}(i)$.

4. Using *NXFit*

NXFit has a graphical user interface (GUI) to enable the user to set the operating parameters easily. Fig. 1 shows a completed example of this GUI in an initialized state ready for a simulation to begin. As can be seen from Fig. 1, the user has to specify the name and path of the various data files and parameter files used in the fitting process and supply other relevant parameters.

[1] *fminsearchcon* was created by John D'Errico of the MATLAB user community and can be freely downloaded from the MATLAB file exchange: http://www.mathworks.co.uk/matlabcentral/fileexchange/8277-fminsearchbnd-fminsearchcon.

A parameter file containing the initial values of R_{ij}, N_{ij} and σ_{ij} for each correlation must be supplied, together with a file containing the constraints for each parameter, *i.e.* how much they can vary during the optimization.

The experimental data should be Fourier transformed according to equation (4). Since *NXFit* generates the pair function $p_{ij}(Q)$ [equation (9)] before Fourier transformation into r space to allow comparison with the experimental $T(r)$, the range over which the experimental data was Fourier transformed and the type of window function used must be specified. If both neutron and X-ray data are to be fitted simultaneously, the relative weighting of the two data sets can be entered.

In order to calculate $T(r)$, *NXFit* needs to know the composition of the sample and the scattering strengths of the atoms present. This information is supplied by the user in the form of a scattering factor file. In the case of neutron data, the scattering factor file contains the atomic number, average neutron scattering length and atomic fraction for each element in the sample. When fitting X-ray data, the neutron scattering length is replaced with the coefficients a_i, b_i and c, which are used to generate the X-ray scattering factors *via* the following equation:

$$f_i(Q) = \sum_i^4 a_i \exp(-b_i s^2) + c, \tag{13}$$

where $s = Q/4\pi$. Values for a_i, b_i and c are tabulated in *International Tables of Crystallography* (Brown *et al.*, 2006) and by Cromer & Mann (1968).

NXFit allows the user to specify the range in r space over which the experimental $T(r)$ is to be simulated and the spacing in Q used when $p_{ij}(Q)$ is generated. When using *NXFit*, it is not usual to fit $T(r)$ beyond 4 Å because the problem of overlapping correlations makes it very difficult to assign features to particular pairs of atoms. The maximum number of iterations to be used in the fitting process can also be specified.

NXFit produces two or three output files depending on how many data sets have been used. These are a $T(r)$ fit file for each data set and a file containing the optimized parameters. The fit contains the original experimental $T(r)$ and the simulated $T(r)$, together with the partial correlation functions that it comprises (*i.e.* the contributions from the individual pairs of atoms).

Like any program, *NXFit* is not without its limitations. Particular care must be taken when preparing the initial parameter file since this is the point at which the user ascribes the various features in $T(r)$ to particular atomic correlations. Mistakes here can lead to nonsensical results later. To help with these assignments, it is often useful to look at the atomic distances present in crystals of similar composition and to examine in the results of studies of similar amorphous samples. It is also beneficial to bring in data from other techniques, for example EXAFS or NMR. Although the setting up of the initial parameters file can be problematic, it does allow for the refinement of parameters for mixed coordination sites, albeit in an indirect manner. If the sample studied contained an element in multiple coordination environments, separate correlations can be set up for each environment and the parameters refined. If the coordination numbers of the sites are known, the relative abundance of each site can be calculated from the observed coordination numbers obtained from the refinement. For example, if a material contained a metal residing in two environments with respect to oxygen, fourfold or sixfold coordination, and the refined coordination numbers for these two correlations came out as 2 and 3, respectively, the calculated occupancy of both sites would be 0.5. The use of this approach has been demonstrated for aluminium-containing phosphate-based glass where aluminium resides in four-, five- and sixfold environments (Smith, King *et al.*, 2013). Good agreement was obtained between neutron diffraction results and those from ^{27}Al NMR.

At present *NXFit* does not calculate the errors associated with the optimized output parameters. However, the robustness of the fit can be tested by fitting the data with different starting parameters and taking the difference between the output parameters obtained from the two fits as estimates of the errors (Barney *et al.*, 2011). This approach has been adopted here in the two examples of the application of *NXFit.*

5. Application to diffraction data from a sodium metaphosphate glass

Phosphate-based glasses have a variety of composition-dependent properties, which have led to their development for a range of speciality applications including nuclear waste containment (Day *et al.*, 1998), fast ion conductors in solid state electrolytes (Bates *et al.*, 1992), hermetic seals (Brow *et al.*, 1995) and high-power lasers (Weber, 1990). Understanding the structure of such materials is therefore very important in optimizing their atomic properties. Here we describe the use of *NXFit* to fit both neutron and X-ray diffraction data from a melt-quenched $(Na_2O)_{0.5}(P_2O_5)_{0.5}$ metaphosphate glass. This material is important because it is both biocompatible and bioresorbable (Knowles, 2003; Abou Neel *et al.*, 2009).

The neutron diffraction data were collected on the GEM diffractometer at the ISIS spallation neutron source at the Ruther-

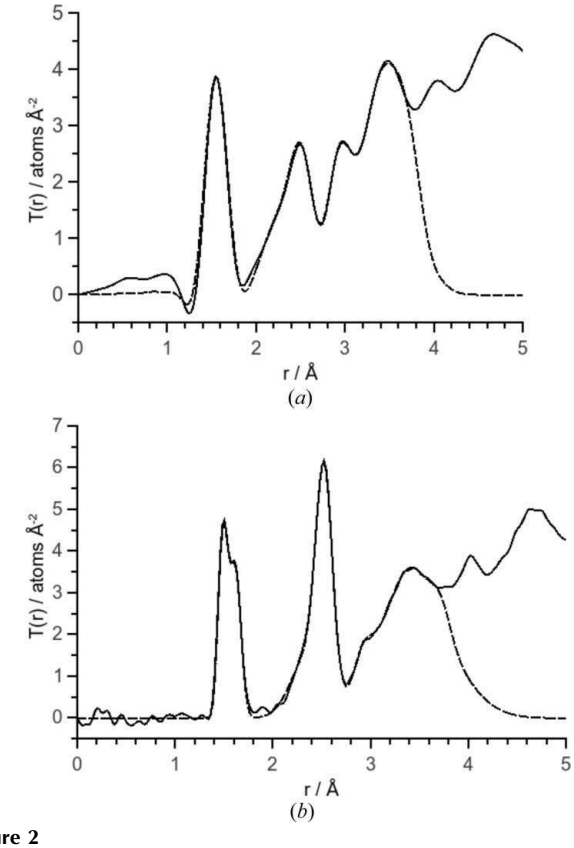

Figure 2
Real-space pair-distribution functions (solid lines) together with their simulations (dashed lines) from $(Na_2O)_{0.5}(P_2O_5)_{0.5}$ metaphosphate glass: (*a*) X-ray diffraction data and (*b*) neutron diffraction data. During the fitting process, the relative weightings of the X-ray and neutron data were 0.4 and 0.6, respectively.

Table 1
Structural parameters obtained from the fitting of the diffraction data using *NXFit*.

R is the atomic separation, *N* the coordination number and σ the disorder parameter. BO denotes a bridging oxygen atom and NBO a nonbridging oxygen atom.

Sample	Correlation	*R* (Å)	*N*	σ (Å)
$(Na_2O)_{0.5}(P_2O_5)_{0.5}$ metaphosphate glass	P—NBO	1.48 (1)	1.7 (1)	0.03 (1)
	P—BO	1.61 (1)	1.9 (1)	0.05 (1)
	Na—O	2.36 (1)	5.0 (1)	0.17 (4)
	O—O	2.52 (1)	3.7 (1)	0.08 (1)
	Na—Na	2.89 (1)	2.2 (3)	0.07 (3)
	P—P	2.95 (1)	2.1 (2)	0.10 (1)
	Na—O	3.20 (7)	2.6 (2)	0.19 (2)
$(TiO_2)_{0.18}(SiO_2)_{0.82}$ sol–gel	O—H	0.99 (1)	0.2 (1)	0.01 (1)
	C—H	1.21 (1)	1.6 (1)	0.05 (1)
	Si—O	1.61 (1)	3.7 (1)	0.04 (1)
	Ti—O	1.82 (2)	2.3 (7)	0.07 (1)
	Ti—O	2.01 (4)	3.7 (10)	0.13 (2)
	Si—H	2.10 (7)	0.6 (1)	0.22 (3)
	O—O	2.64 (1)	3.6 (1)	0.09 (1)
	O—O	2.94 (3)	1.2 (2)	0.17 (1)
	Si—Si	3.08 (2)	2.0 (10)	0.10 (1)
	Ti—Si	3.13 (4)	2.6 (7)	0.09 (3)
	Ti—Ti	3.15 (8)	3.2 (7)	0.21 (3)

ford Appleton Laboratory, UK. Further details of the sample preparation and collection and analysis of the neutron diffraction data are given by Pickup *et al.* (2007). The X-ray diffraction data were collected in transmission geometry on Station 9.1 at the SRS, Daresbury Laboratory, UK. The data were corrected using a series of MATLAB programs written in-house, which were themselves based on the method of Warren (1990).

Fig. 2 shows neutron and X-ray $T(r)$ curves from $(Na_2O)_{0.5}$-$(P_2O_5)_{0.5}$ glass that have been fitted simultaneously using *NXFit*. The refined parameters used to generated these fits are given in Table 1. These parameters are in general agreement with those from the previous neutron study of $(Na_2O)_{0.5}(P_2O_5)_{0.5}$ (Pickup *et al.*, 2007). There are a few small differences; these are mainly due to the inclusion of the X-ray data and to changes to the assignment of some of the features in $T(r)$. In the previous work O—O and Na—Na correlations at 2.82 and 3.07 Å, respectively, were used in the fitting process, whereas in the present study these correlations were replaced by an Na—Na distance of 2.89 Å and a second nearest-neighbour Na—O distance of 3.20 Å. These changes were made on the basis of recent RMC modelling studies of metaphosphate glasses. Unpublished work by the authors suggests the Na—Na nearest-neighbour distance to be 2.9 Å and the second nearest-neighbour Na—O distance to be 3.0 Å. A study of $(CaO)_{0.5}(P_2O_5)_{0.5}$ glass by Wetherall *et al.* (2009) also identified a long metal–oxygen distance of

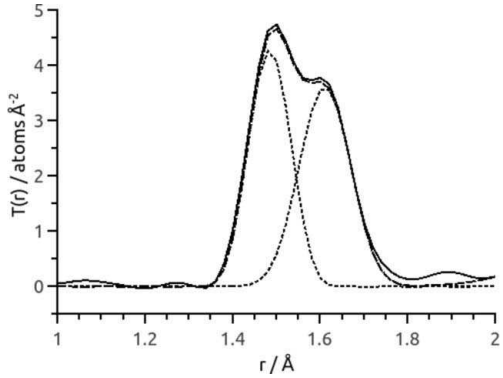

Figure 3
Neutron $T(r)$ from $(Na_2O)_{0.5}(P_2O_5)_{0.5}$ metaphosphate glass in the region of the P—O correlation showing the contributions from P—NBO bonds at 1.49 Å and P—BO bonds at 1.61 Å.

~3 Å in models that were consistent with both neutron and X-ray data. Despite this careful assignment of the Na—O correlation, the refined distance in Table 1 is longer than that from the RMC model. This is probably due to the problem of overlapping correlations at 3 Å and above and highlights one of the limitations of *NXFit*. There will be longer correlations that cannot be accurately modelled by *NXFit* yet still contribute to the intensity of $T(r)$ in this region. Given this, the refined parameters for the Na—O correlation should be treated with a degree of caution.

The accepted model for metaphosphate glasses is long chains of PO_4^{3-} tetrahedra held together by electrostatic forces between the negative charges on the nonbridging oxygen atoms (NBOs) of the phosphate groups and the cations (Hoppe, 1996; Hoppe *et al.*, 2000). Each phosphate group is expected to have two NBOs and two bridging oxygen atoms (BOs). Since the PO_4^{3-} tetrahedra are arranged in chains, each phosphorus atom is expected to have two phosphorus neighbours across the BOs. These key features are reflected in the parameters in Table 1: the P—BO and P—P coordination numbers are 2 within experimental error and the P—NBO coordination number is close to two. Furthermore, fitting with *NXFit* also identifies some of the more subtle features of the metaphosphate glass structure. The neutron data were collected over a wide Q range ($Q_{max} \simeq 60$ Å^{-1}), which results in excellent real-space resolution and allows the distinct P—NBO and P—BO distances to be resolved. This is illustrated by Fig. 3, which shows the contributions of the P—NBO and P—BO partial correlation functions to the neutron $T(r)$ in the range 1–2 Å as output by *NXFit*. The P—NBO bond distance is shorter than the P—BO bond length because the former has a degree of double-bond character (Hoppe *et al.*, 2000). The other interesting feature of the structure of $(Na_2O)_{0.5}(P_2O_5)_{0.5}$ becomes clear if the number of NBOs per Na^+ is considered alongside the Na—O coordination number. The former is 2 and the latter, as determined here and in excellent agreement with the previous study by Hoppe *et al.* (1995), is 5. Assuming the sodium ions coordinate preferentially with the negatively charged NBOs, there are not enough NBOs to satisfy the preferred coordination geometry of the sodium ions unless the NBOs are shared between these ions. This sharing leads to the relatively short Na—Na nearest-neighbour distance that is observed here and in previous studies (Hoppe *et al.*, 2000; Pickup *et al.*, 2007).

6. Application to diffraction data from a sol–gel-derived TiO_2–SiO_2 glass

Titania–silica mixed oxide glasses have properties that are useful for a number of applications. Such examples are as ultra-low thermal expansion glasses (Scherer & Brinker, 1990), thin films with tailored refractive indices (Schultz & Smyth, 1972) and catalysts (Davis & Liu, 1997; Imamura *et al.*, 1995; Holland *et al.*, 2000; Beck *et al.*, 2001).

The data presented here are from a $(TiO_2)_{0.18}(SiO_2)_{0.82}$ sol–gel sample that has been heated to 523 K. The diffraction data were collected as part of a wider neutron diffraction with isotopic substitution study of the titanium environment in sol–gel TiO_2–SiO_2 materials (Pickup, Sowrey, Newport *et al.*, 2004). The sample preparation and collection of the neutron diffraction data are described therein. The X-ray diffraction data were again collected on Station 9.1 at the SRS and analysed in the same manner as the data described in §5.

Fig. 4 shows the $T(r)$ curves from the $(TiO_2)_{0.18}(SiO_2)_{0.82}$ sol–gel together with their simulations from *NXFit*. The output parameters from the fitting process are given in Table 1. The quality of the fits shown in Fig. 4 is not as good as that achieved for the melt-quenched

sodium metaphosphate glass. This is due to the complexity of sol–gel glasses compared with simple oxide glasses. Sol–gel materials such as the one studied here contain carbon and hydrogen in addition to their oxide components, and their composition can change over time as they age; this makes it difficult to correct diffraction data. The low-r regions ($r < 0.8$ Å) of the curves in Fig. 4 are not flat, indicating that the corrections to the data have not worked as well as they have for the data shown in Fig. 2. Furthermore, it is known that TiO_2–SiO_2 sol–gel glasses can reversibly absorb moisture (Mountjoy *et al.*, 1999). Since the neutron diffraction data were collected under vacuum whereas the X-ray data were collected at ambient pressure, there remains the possibly that the low pressure could have partially dehydrated the sample during the neutron diffraction measurement, resulting in an altered composition. Despite these limitations, the key features of the structure of sol–gel $(TiO_2)_{0.18}(SiO2)_{0.82}$ can be obtained from the data in Fig. 4. The Si—O coordination number is close to 4, as expected for a silicate-based material consisting of a network of SiO_4 tetrahedra (Wright, 1994). Two Ti—O distances are observed, at 1.82 and 2.01 Å, respectively, with an overall Ti—O coordination number of 6. In agreement with previous studies (Mountjoy *et al.*, 1999; Pickup, Sowrey, Newport *et al.*, 2004), these results are consistent with titanium predominantly occupying a distorted octahedral environment with two short Ti—O and four long Ti—O bonds. The nearest-neighbour O—O and Si—Si distances of 2.64 and 3.08 Å, respectively, are typical of those found in vitreous silica (Wright, 1994). In a fully densified SiO_2 network, the O—O and Si—Si coordination numbers are 6 and 4, respectively. Here those numbers are 3.6 and 2.0, reflecting the fact that the sol–gel is only a partially condensed silica network, which is further disrupted by the presence of TiO_2. A second O—O distance is also observed, at 2.94 Å, and is assigned to an O—O distance associated with TiO_x polyhedra (Pickup, Sowrey, Newport *et al.*, 2004). The large value of σ for this correlation, of 0.17 Å, reflects the high degree of disorder associated with the titanium environment. The Ti—Ti distance of 3.15 Å observed here agrees well with that determined for a sample with the same Ti/Si ratio but heat treated to 1023 K (Pickup, Sowrey, Drake *et al.*, 2004). In order to achieve a satisfactory fit to the neutron data, it was necessary to include O—H, C—H and Si—OH correlations, providing further evidence that the structure is not fully consolidated after heating to 523 K. Note that these correlations have little effect on the fit to the X-ray data because hydrogen is such a weak scatterer of X-rays.

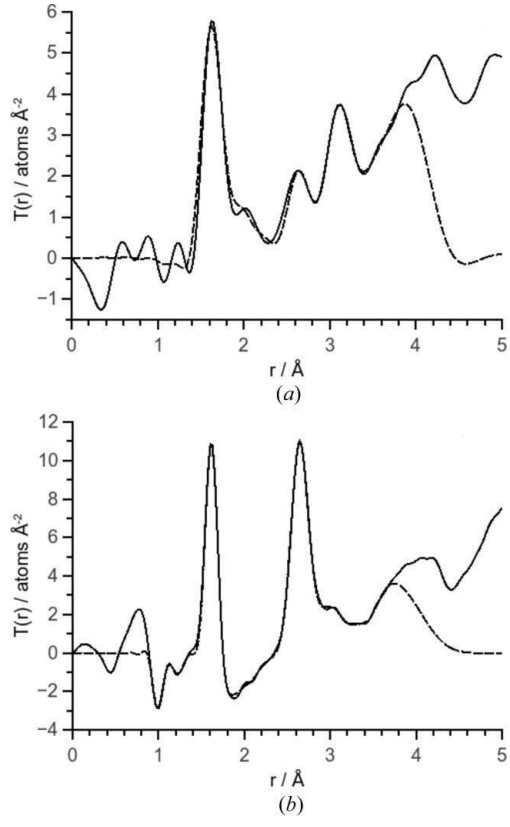

Figure 4
Real-space pair-distribution functions (solid lines) together with their simulations (dashed lines) from $(TiO_2)_{0.18}(SiO_2)_{0.82}$ sol–gel: (*a*) X-ray diffraction data and (*b*) neutron diffraction data. During the fitting process, the relative weightings of the X-ray and neutron data were 0.4 and 0.6, respectively.

7. Application of *NXFit* to the study of other materials

Other examples of the utilization of *NXFit* in the analysis of diffraction data from a wide range of materials can be found in the literature. Examples of such materials include bioactive glasses (Martin *et al.*, 2012; Smith, Martin *et al.*, 2013), Ca–Mg–Cu metallic glasses (Barney *et al.*, 2011) and amorphous iron phosphate (Al-Hasni *et al.*, 2013).

8. Conclusions

NXFit is a program capable of simulating the pair-distribution functions from amorphous materials. Partial correlation functions are generated in Q space, summed and Fourier transformed to $T(r)$ for comparison with the experimental data in r space. Coordination numbers, atomic separations and disorder parameters are all varied (within user-defined limits) until a satisfactory fit to the experimental data has been obtained. When fitting both neutron and X-ray data simultaneously it is possible to weight one data set relative to the other. The application of *NXFit* to the fitting of neutron and X-ray data from a melt-quenched $(Na_2O)_{0.5}(P_2O_5)_{0.5}$ glass and $(TiO_2)_{0.18}$-$(SiO_2)_{0.82}$ sol–gel has been demonstrated here.

The authors wish to acknowledge the STFC (CMPC06103) and the EPSRC (EP/C000714/1, EP/C004671/1 and EP/C515560/1) for funding and the use of the EPSRC Chemical Database Service at the STFC Daresbury Laboratory. They would also like to thank Dr Emma Barney and Dr Alex Hannon of the Rutherford Appleton Laboratory for their input to the development of *NXFit*.

References

Abou Neel, E. A., Pickup, D. M., Valappil, S. P., Newport, R. J. & Knowles, J. C. (2009). *J. Mater. Chem.* **19**, 690–701.
Alder, B. J. & Wainwright, T. E. (1959). *J. Chem. Phys.* **31**, 459–466.
Al-Hasni, B. M., Mountjoy, G. & Barney, E. (2013). *J. Non-Cryst. Solids*, **380**, 141–152.
Barney, E. R., Hannon, A. C., Senkov, O. N., Scott, J. M., Miracle, D. B. & Moss, R. M. (2011). *Intermetallics*, **19**, 860–870.
Bates, J., Dudney, N., Gruzalski, G., Zuhr, R., Choudhury, A., Luck, C. & Robertson, J. (1992). *Solid State Ionics*, **53–56**, 647–654.
Beck, C., Mallat, T., Brgi, T. & Baiker, A. (2001). *J. Catal.* **204**, 428–439.
Brow, R., Kovacic, L. & Loehman, R. (1995). *Ceram. Trans.* **70**, 177–187.
Brown, P. J., Fox, A. G., Maslen, E. N., O'Keefe, M. A. & Willis, B. T. M. (2006). *International Tables for Crystallography*, Vol. C, *Mathematical, Physical and Chemical Tables*, 1st online ed., edited by E. Prince, pp. 554–595. Chester: International Union of Crystallography.
Bruni, S., Cariati, F., Corrias, A., Gaskell, P. H., Lai, A., Musinu, A. & Piccaluga, G. (1995). *J. Phys. Chem.* **99**, 15229–15235.
Cormack, A. & Cao, Y. (1996). *Mol. Eng.* **6**, 183–227.

Cromer, D. T. & Mann, J. B. (1968). *Acta Cryst.* A**24**, 321–324.
Davis, R. J. & Liu, Z. (1997). *Chem. Mater.* **9**, 2311–2324.
Day, D., Wu, Z., Ray, C. & Hrma, P. (1998). *J. Non-Cryst. Solids*, **241**, 1–12.
Farrow, C. L., Juhas, P., Liu, J. W., Bryndin, D., Boin, E. S., Bloch, J., Proffen, T. & Billinge, S. J. L. (2007). *J. Phys. Condens. Matter*, **19**, 335219.
Hannon, A. C., Barney, E. R., Holland, D. & Knight, K. S. (2008). *J. Solid State Chem.* **181**, 1087–1102.
Hannon, A. C., Howells, W. S. & Soper, A. K. (1990). *Inst. Phys. Conf. Ser.* **107**, 193–211.
Holland, M. A., Pickup, D. M., Mountjoy, G., Tsang, E. S. C., Wallidge, G. W., Newport, R. J. & Smith, M. E. (2000). *J. Mater. Chem.* **10**, 2495–2501.
Hoppe, U. (1996). *J. Non-Cryst. Solids*, **195**, 138–147.
Hoppe, U., Stachel, D. & Beyer, D. (1995). *Phys. Scr.* T**57**, 122–126.
Hoppe, U., Walter, G., Kranold, R. & Stachel, D. (2000). *J. Non-Cryst. Solids*, **263–264**, 29–47.
Imamura, S., Nakai, T., Kanai, H. & Ito, T. (1995). *J. Chem. Soc. Faraday Trans.* **91**, 1261–1266.
Keen, D. A. (2001). *J. Appl. Cryst.* **34**, 172–177.
Knowles, J. C. (2003). *J. Mater. Chem.* **13**, 2395–2401.
Lagarias, J., Reeds, J., Wright, M. & Wright, P. (1998). *SIAM J. Control*, **9**, 112–147.
Lorch, E. (1969). *J. Phys. C Solid State Phys.* **2**, 229–237.
Martin, R. A., Moss, R. M., Lakhkar, N. J., Knowles, J. C., Cuello, G. J., Smith, M. E., Hanna, J. V. & Newport, R. J. (2012). *Phys. Chem. Chem. Phys.* **14**, 15807–15815.
McGreevy, R. L. (2001). *J. Phys. Condens. Matter*, **13**, R877–R913.
McGreevy, R. L. & Pusztai, L. (1988). *Mol. Simul.* **1**, 359–367.
McKinnon, K. (1998). *SIAM J. Control*, **9**, 148–158.
Mountjoy, G., Pickup, D., Wallidge, G., Cole, J., Newport, R. & Smith, M. (1999). *Chem. Phys. Lett.* **304**, 150–154.
Nelder, J. A. & Mead, R. (1965). *Comput. J.* **7**, 308–313.
Pickup, D. M., Ahmed, I., Guerry, P., Knowles, J. C., Smith, M. E. & Newport, R. J. (2007). *J. Phys. Condens. Matter*, **19**, 415116.
Pickup, D., Sowrey, F., Drake, K., Smith, M. & Newport, R. (2004). *Chem. Phys. Lett.* **392**, 503–507.
Pickup, D. M., Sowrey, F. E., Newport, R. J., Gunawidjaja, P. N., Drake, K. O. & Smith, M. E. (2004). *J. Phys. Chem. B*, **108**, 10872–10880.
Pings, C. J. & Waser, J. (1968). *J. Chem. Phys.* **48**, 3016–3018.
Rietveld, H. M. (1969). *J. Appl. Cryst.* **2**, 65–71.
Scherer, G. & Brinker, C. (1990). *Sol–Gel Science: the Physics and Chemistry of Sol–Gel Processing*. Academic Press: San Diego.
Schultz, P. & Smyth, H. (1972). *Amorphous Materials*. London: Wiley.
Smith, J. M., King, S. P., Barney, E. R., Hanna, J. V., Newport, R. J. & Pickup, D. M. (2013). *J. Chem. Phys.* **138**, 034501.
Smith, J. M., Martin, R. A., Cuello, G. J. & Newport, R. J. (2013). *J. Mater. Chem. B*, **1**, 1296–1303.
Soper, A. K. (2001). *Mol. Phys.* **99**, 1503–1516.
Soper, A. K. (2005). *Phys. Rev. B*, **72**, 104204.
Warren, B. E. (1990). *X-ray Diffraction.* New York: Dover.
Weber, M. (1990). *J. Non-Cryst. Solids*, **123**, 208–222.
Wetherall, K. M., Pickup, D. M., Newport, R. J. & Mountjoy, G. (2009). *J. Phys. Condens. Matter*, **21**, 035109.
Wright, A. C. (1985). *J. Non-Cryst. Solids*, **76**, 187–210.
Wright, A. C. (1994). *J. Non-Cryst. Solids*, **179**, 84–115.
Yarker, C. A., Johnson, P. A., Wright, A. C., Wong, J., Greegor, R. B., Lytle, F. W. & Sinclair, R. N. (1986). *J. Non-Cryst. Solids*, **79**, 117–136.